Open access • Journal Article • DOI:10.1016/J.IJREFRIG.2009.05.008

Design and simulation of a heat pump for simultaneous heating and cooling using HFC or CO2 as a working fluid — Source link

Paul Byrne, Jacques Miriel, Yves Lénat

Institutions: Intelligence and National Security Alliance

Published on: 01 Nov 2009 - International Journal of Refrigeration-revue Internationale Du Froid (Elsevier)

Topics: Air source heat pumps, Heat pump, Coefficient of performance, Heat exchanger and Refrigerant

Design and simulation of a heat pump for simultaneous heating and cooling using HFC or CO2 as a working fluid

Paul Byrne, Jacques Miriel, Yves Lénat

Design and simulation of a heat pump for simultaneous heating and cooling using HFC or CO_2 as a working fluid

Paul **BYRNE**, Jacques **MIRIEL**, Yves **LENAT**

paul.byrne@univ-rennes1.fr

Equipe MTH – Laboratoire LGCGM - INSA de Rennes

20 avenue des buttes de Coësmes - CS 14 315 - 35 043 Rennes Cedex – France

Tel: +33 2 23 23 42 97

Fax: +33 2 23 23 40 51

ABSTRACT

This article presents a Heat Pump for Simultaneous heating and cooling (HPS) designed for hotels, luxury dwellings and smaller office buildings. The main advantage of the HPS is to carry out simultaneously space heating and space cooling in a dual mode. The ambient air is used as a balancing source to run a heating or a cooling mode. The HPS also participates to domestic hot water preparation all year round. The second advantage is that, during winter, some energy recovered by subcooling of the refrigerant is stored at first in a cold water tank that is not used for cooling. This energy is used subsequently as a cold source at the water evaporator in order to improve the average coefficient of performance and to run a defrosting sequence at the air evaporator. Two refrigerants are studied: HFC R407C and carbon dioxide. HFCs provide good performance, but new restrictive regulations on F-gases lead us to study low-GWP refrigerants as well. Highly efficient models of compressors and heat exchangers have been defined. Annual simulations show that CO_2 is a refrigerant which adapts rather well to the operation of the HPS thanks to the higher amount of energy available by subcooling and the large temperature glide at heat rejection used for DHW production.

Keywords: *design, simulation, heating, cooling, domestic hot water, HFC, R407C, CO_2*

NOMENCLATURE

c	relative clearance volume (-)
C	electricity consumption (Wh)
Cp	specific heat (J kg^{-1} K^{-1})
h	enthalpy (kJ kg^{-1})
HP	high pressure (Pa)
L	latent heat (J kg^{-1})
LP	low pressure (Pa)
m	mass (kg)
$\dot{m}$	mass flow rate (kg s^{-1})
n	polytropic exponent (-)
q	heating or cooling load (Wh)
$\dot{Q}$	heating or cooling capacity (W)
r	ratio (-)
t	time (s)
T	temperature (°C)
x_L	percentage of cooling capacity used for defrosting (%)
V_s	swept volume (m^3 s^{-1})
$\dot{W}$	compression work (W)

Greek symbols:

η	efficiency (-)
ρ	density (kg m^{-3})

Subscripts:

c	cooling
CM	cooling mode
cs	cold source
df	defrosting
DM	dual mode
el	electric
f	frost or with frosting

F	fusion
h	heating
HM	heating mode
HP	heat pump
i	in
is	isentropic
mec	mechanical
nof	without frosting
o	out
r	refrigerant
S	sublimation
sc	subcooling
vol	volumetric
w	water

1. Context and objectives

Nowadays, global warming being a major concern for the environment, researchers are focussing more and more on energy efficiency in buildings. In developed countries, commercial and residential buildings account for around 40% of national energy consumption and 25% of green house gas emissions. This is the sector in which energy savings can be the highest and building companies are proposing new environmentally-friendly constructions. Thermal performance of buildings is thus continuously improving. Moreover, comfort requirements demand more and more energy. Indeed, whilst domestic hot water (DHW) demands continue to increase, the demand for cooling is rising to compensate internal heat gains caused by more and more household electrical equipment. Also a better thermal envelope implies that new buildings need less energy for heating and more for cooling. Therefore thermal needs of new buildings are more balanced between heating and cooling over the year.

During winter, energy is demanded exclusively for space heating and DHW production. Between winter and summer, some buildings can demand simultaneously cooling in rooms facing south and heating in rooms facing north. During summer, energy is needed for DHW production and space cooling

at the same time. An answer to a dual energy demand is the heat pump, since it has simultaneously a heating capacity at the condenser and a cooling capacity at the evaporator.

This study presents the reasoning behind the design of a heat pump that can satisfy fluctuating needs, simultaneous or not, in heating and cooling. This heat pump is named HPS (Heat Pump for Simultaneous heating and cooling) and can be installed in hotels where DHW demands are high and glass fronted buildings where simultaneous needs in space heating and space cooling are more frequent. The first objective is to produce, as much as possible, heat and cold using the same energy input at the compressor. The second objective is to limit the performance loss of air-source heat pumps during winter due to low air temperatures and frosting (Liu et al., 2007).

The design depends on the working fluid. The refrigerants used in new heat pumps are HFCs and natural fluids. HFCs provide good performances, but these fluids are classified by the Kyoto Protocol (1997) in the category of green house gases. That is why they are likely to be banned in the future. As far as mobile air conditioning is concerned, European Directives already plan the phase-out of refrigerants having a 100-year GWP (Global Warming Potential) over 150 kg_{CO2} by 2011. Among natural fluids (GWP $\leq$ 1 kg_{CO2} over 100 years) carbon dioxide (CO_2, R744) seems one of the most adapted to residential applications or offices because it fulfils the requirements of low toxicity and low flammability. According to Lorentzen (1994, 1995), author of "Revival of carbon dioxide as a refrigerant", CO_2 is the most promising natural refrigerant as a substitute for HCFCs and HFCs. In Japan, CO_2 heat pump water heaters called “Ecocute” are now commonly used (Kusakari, 2006). According to Nekså (2002, 2008), carbon dioxide is a very promising fluid for space heating applications.

Faced with this context, we have built numerical models and run simulations with highly efficient compressors and heat exchangers models to evaluate the performance of a HPS and compared the results to those of a standard reversible heat pump. Also, the possibility of using carbon dioxide instead of a HFC has been examined. The comparisons have been led from technical and environmental points of view. The HFC chosen for the simulation study is R407C, a working fluid widely used in heat pumping technology.

2. Design of the HPS

Heat exchangers

The HPS (Fig. 1 and Fig. 2) has three main heat exchangers: a condenser (or a gas cooler for carbon dioxide) that heats a water tank for space heating; an evaporator that cools a second water tank for space cooling; and a balancing air coil that works either as a condenser in a cooling mode or an evaporator in a heating mode. The latter is a three-fluid heat exchanger working with air on one side and on the other side, refrigerant flowing through two separate networks of tubes for high and low pressure. A subcooling heat exchanger is added to the three heat exchanger configuration. It enables energy storage on the cold water loop when it is not used for cooling, mainly during winter. The amount of energy stored is used to run the water evaporator during a subsequent mode of operation. Most of the time during winter, working on water instead of air at evaporation lifts up the evaporating temperature as well as the low pressure and so, it improves the performance of the heat pump. Moreover this technique liberates the air coil for defrosting without stopping the heat production.

Operating modes

The operation of the HPS is based upon three main modes: a cooling mode using the water evaporator and the air heat exchanger as a condenser; a dual mode preparing simultaneously hot and cold water using the water heat exchangers (condenser and evaporator); and a heating mode using the water condenser, the subcooler for heat storage on the cold water loop and the air coil as an evaporator. Commutation of modes is managed by a programmable controller that opens or closes the appropriate on-off electronic valves.

HFC configuration

The HFC HPS (Fig. 1) is equipped with a standard plate condenser producing hot water for space heating. The controller does not adapt the condensing temperature to DHW preparation since the priority application of the HPS is space heating and because it would degrade too much the performance. Thus domestic hot water is prepared using an extra heat exchanger placed on the pipe between the outlet of the condenser and the hot water tank. Then an auxiliary heater brings the water to the appropriate temperature for domestic use. Graphs a1, a2 and a3 of Fig. 3 show the HFC HPS heat production processes on temperature – enthalpy charts. Each graph shows the temperature evolutions of the refrigerant (plain lines), of the hot or cold tank water (dotted lines) and the DHW (doubled and dotted lines) in the high pressure heat exchangers. Enthalpy is only linked to the refrigerant state at inlets and outlets of heat exchangers. Heat exchangers being counter-flow, the water inlet (respectively outlet) corresponds to the

refrigerant outlet (resp. inlet). On the chart, the inlet (or outlet) point for water corresponds to the water temperature and to the refrigerant enthalpy at that point of the heat exchanger. For HFC charts, DHW is not produced by the condensers. DHW temperature evolutions are represented under the outlet of the condenser. In all modes, condensation energy is used to heat the hot water tank. The DHW is first preheated through an exchanger by the hot water for space heating and then reheated by an auxiliary heater. The cold water tank is heated using the subcooling energy of the refrigerant in the heating mode (graph a1). The cooling mode is standard. It uses the water evaporator and the air coil as a condenser.

CO_2 configuration

The main difference between the HFC and CO_2 machines resides in the heat exchangers technology so that it can withstand operating pressures above 100 bar. The CO_2 HPS (Fig. 2) uses the transcritical cycle of carbon dioxide in which heat rejection occurs at a pressure above the critical point. The water condenser in the HFC configuration corresponds to a gas cooler in the CO_2 configuration. The most efficient CO_2 heat exchangers are made up of microchannels. They can handle high pressures and provide higher heat transfer coefficients (Zhao et al., 2001). The gas cooler is divided into three sections. The top section is used for domestic hot water preparation at 55-60°C. The middle section is dedicated to the production of hot water for space heating at temperatures between 25 and 45°C. Finally, the lower section is connected to the cold water tank for energy storage during winter. Stene (2005) proposes to use the lower part of the gas cooler (at the lower temperature) to preheat DHW, the middle part to heat water for space heating and the upper part to reheat DHW. This could not be done simply with the CO_2 HPS since the energy storage on the cold loop, by subcooling of the refrigerant, is a key feature of the machine. Graphs b1, b2 and b3 of Fig. 3 show the heat production processes of the CO_2 HPS. The DHW is heated using the top section of the gas cooler in which the temperatures are the highest. During summer in the dual mode, this section of the gas cooler is the only one used (graph b3). The middle section is dedicated to space heating in the heating mode and the winter dual mode (graphs b1 and b2). The cold water tank is heated using the subcooling energy of the refrigerant in the heating mode (graph b1).

The transcritical cycle of CO_2 provides a high temperature at the gas cooler inlet and a continuous temperature glide along the gas cooler, which enables the production of hot water for domestic use as required for the HPS. For this reason, even if it provides poorer performance than standard cycles with HFCs, the CO_2 transcritical cycle seems to suit the residential and office applications selected for the

HPS. Also, the defrosting technique benefits from the high amount of energy recoverable by subcooling (about 30% of the total energy available at heat rejection).

Cooling and dual mode during summer

During summer, the dominant mode is the cooling mode. When there are needs for DHW, the dual mode is run until the demand is satisfied. The HPS then switches back to the cooling mode.

All modes during in-between seasons

Between summers and winters, the heating and cooling needs are lower and fluctuating. The HPS produces hot and cold water mainly in the dual mode to be able to provide energy for any demand.

Alternated sequence during winter period

During winter, the HPS alternates between heating mode and dual mode in order to use to a maximum the water evaporator instead of the air evaporator. In the heating mode, the subcooling of the refrigerant is used to heat the cold tank. The cold tank temperature increases from 5 to 15°C. The HPS then changes mode and operates in the dual mode. The controller stops the fan of the air evaporator and switches the on-off electronic valves in order to use the water evaporator instead of the air evaporator. The subcooler is bypassed by changing the position of the three-way valve and becomes inactive. The cold tank being the cold source for the water evaporator, its temperature decreases from 15 to 5°C. Then the controller switches the HPS back to the heating mode and a new sequence starts again. This alternated sequence enables a continuous production of heat for space heating using, during part of the time, a cold source at a temperature higher than that of a standard heat pump. Using this alternated sequence, the average performance can be improved during winter.

Defrosting technique

Defrosting is carried out during the second part of the alternated winter sequence. In the heating mode, under cold outside air temperatures, the fins of the air evaporator get frosted. Before the frost thickness becomes critical, the cold tank temperature has raised 15°C and the dual mode has been engaged. In the dual mode, the air coil is automatically defrosted. After flowing through the water condenser, the refrigerant enters the three-fluid heat exchanger at a temperature around 30°C and is subcooled by heat exchange with the frosted fins. At the same time, a thermosiphon forms between the two evaporators. Part of the vapour coming out of the water evaporator migrates towards the air

evaporator where the temperature, and thus the pressure, is lower. The gas exchanges heat with the frosted fins and condenses. Finally, it flows back to the water evaporator by gravity. The sequence finishes in the dual mode until the cold tank temperature decreases back to 5°C.

A major advantage of this operating sequence is to carry out defrosting without stopping or even degrading the heat production. Frost thickness can thus be minimized and mean convection heat transfer coefficients at the evaporator can be maximized (Xia et al., 2006). The average efficiency in heating is improved compared to the performance of heat pumps that use hot gas or reversed cycle defrosting methods.

High pressure control

As pressures and temperatures are linked during condensation, high pressure control ensures that condensation occurs in the appropriate condenser. Moreover it is able to control the condensation temperature and thus the heating capacity. A special liquid receiver is placed on the liquid line. It is connected to the compressor discharge line and the inlet of the air evaporator by pipes of smaller diameter on which electronic on-off valves are located (Evr1 and Evr2 on Fig. 1 and Fig. 2).

The high pressure control system indirectly controls the volume of liquid in the receiver. The volume of liquid in the different condensers depends on the mode. If the chosen mode is the heating mode, condensation occurs in the water condenser. The controller calculates the set point for high pressure so that condensation is completed in the condenser. The receiver is filled up with gas coming from the compressor discharge line at a pressure higher than the pressure in the receiver until the calculated pressure is reached. The gas entering the receiver drives the liquid towards the air condenser, the subcooling heat exchanger and the bottom part of the water condenser. If however the chosen mode is the cooling mode, the condenser becomes the air heat exchanger. The set point for pressure is then the lowest possible. The pressure is reduced by driving the gas out of the receiver towards the inlet of the air evaporator. The refrigerant in a liquid phase is sucked out of the water condenser and the subcooler and enters the receiver.

This system is essential to ensure that the air coil and the subcooling heat exchanger are full of liquid and that the condensation is completed in the water condenser during a heating or a dual mode. Otherwise part of the refrigerant could condense in the subcooling heat exchanger and all the energy available from the condensation would not be transferred to the hot water tank for space heating.

The proper operation of the control system depends upon a special liquid receiver being designed quite high and quite narrow with the main objective to enhance temperature stratification and to limit as far as possible thermal transfer between the gas and the liquid. When the gas is injected, part of it condenses. When gas is rejected to the low pressure, part of the liquid evaporates. Although these phenomena can reduce the efficiency of the liquid variation in the receiver, it can stabilize the control system. The receiver is also thermally insulated to reduce the heat transfer with the ambience.

3. Numerical model

Simulation Tools

The numerical approach is carried out in four steps. A first simulation using TRNSYS software is run to obtain the heating, cooling and DHW demands of a standard hotel of 45 bedrooms. In parallel, the steady state performance in heating and cooling is calculated for each mode (heating, cooling and dual modes). The simulation tool used for this calculation is also TRNSYS. Every component of the machine is programmed as a model in FORTRAN and the refrigeration cycle is modelled as the connection of the different components using the input and output variables. The heating sequence alternating heating and dual mode is then studied. Operating times for each mode were calculated during a frosting – defrosting sequence. The last step consists in coupling the demands with the heating and cooling capacities of the heat pump depending on the outside air temperature. This simulation enables to calculate the daily operating times of each working mode and the average daily and annual performance.

Building model

A hotel of 45 bedrooms was modelled. High domestic hot water consumption, thermal zones, wall materials, glazed surfaces, solar protections and ventilation, occupancy and lighting schedules were defined using the building module of TRNSYS so as to calculate the hotel's daily needs in heating and cooling. This simulation was run using the annual weather data file of Paris.

Heat pump models

Four models corresponding to four operating modes (heating mode, cooling mode and dual mode with and without defrosting) were defined to calculate the steady state heating and cooling capacities and

coefficients of performance. Pressure drops and heat losses to the environment are assumed negligible and compressors are modelled using high efficiency factors.

Each mode establishes the performance of the cycle for ambient temperatures varying from -15 to 15°C in heating and from 25 to 40°C in cooling. The cold water is cooled from 10 to 5°C. The set point for space heating water temperature follows a heating curve depending on ambient temperature (Fig. 4). Because of the heating curve, the system performance is always linked to the ambient air temperature, even in the dual mode.

Heat exchanger models

The HFC heat exchangers models use the Log Mean Temperature Difference (LMTD) method. The heat transfer coefficients and the steady state capacities are calculated using the geometrical characteristics of existing heat exchangers (Table 1), the McAdams correlations described in the ASHRAE Handbook Fundamentals (1989) for sensible heat transfers and condensation and the Tran et al. (1996) correlation for boiling heat transfer in the evaporator. The heating and cooling capacities are deduced from the heat transfer coefficients.

The Number of Transfer Units (NTU) and the LMTD calculation methods are used respectively in the CO_2 gas cooler and evaporator. The correlations used to calculate the heat transfer coefficients for carbon dioxide are the Gnielinski correlation (Sarkar et al., 2006) in the gas cooler and the Bennet-Chen correlation in which the nucleate boiling coefficient has been modified by Hwang et al. for carbon dioxide in the evaporator (Haberschill et al., 2007). To calculate heat transfer coefficients for water and CO_2 sensible heat transfer, the McAdams correlations are used (ASHRAE, 1989). As flow boiling for CO_2 is still an issue, another heat transfer correlation, the Wattelet-Carlo correlation (Sarkar et al., 2006) has been tested and showed a negligible variation in the temperature chart (Fig. 5) and the cooling capacity (less than 10% difference).

Condensers and evaporators are divided into zones. Each zone is related to a fraction of the total surface of the exchanger. HFC and CO_2 evaporators have a two-phase zone for evaporation and a single-phase zone for superheating. The HFC condenser has a single-phase zone for desuperheating, a two-phase zone for condensation and another single-phase zone for subcooling. The CO_2 gas cooler and evaporator are divided into 50 sections to take into account the dramatic variations of thermodynamic properties in supercritical conditions. Fig. 6 shows the influence of the number of sections on the simulated

temperature evolutions along a CO_2 evaporator. The temperatures calculated for a 50-section evaporator are near to the temperatures of a 75-section one while significantly diminishing the calculation time.

For all heat exchangers, iterative calculation progresses from section to section from one end of the exchanger to the other. Fig. 7 shows an example of the calculation strategy for an evaporator. In the beginning, on each section or zone, outlet temperatures are set at the inlet values. Then, the calculations use the inlet and outlet temperatures and the structural parameters of the heat exchanger (hydraulic diameter, plate thickness…) to determine the heat transfer coefficients, the new outlet temperatures, the heating and cooling capacities. The outlet variables of a zone are the inlet variables of the next zone. Once the calculation has reached the last zone, it starts again in the other way to the first zone. The whole calculation is iterated until the outlet temperatures of the refrigerant and the other fluid (water or air) have converged for the entire heat exchanger.

Compressor model

The compressor model calculates the mass flow rate and the compression work knowing the input and output pressures (Eq. (1) to (4)) and using the Refprop database (2002). The volumetric efficiency (Eq. (1)) is calculated using a constant polytropic exponent of 1.076 for R407C. This value of the polytropic exponent has been calculated using experimental results carried out in our laboratory on a Copeland ZB38KCE scroll compressor. A brief sensitivity analysis showed that a variation of ± 0.1 of the polytropic exponent value would provoke a variation of the heating COP inferior to 1.4% on a range of pressure ratios from 1.5 to 5. For CO_2, the volumetric efficiency is obtained by a polynomial correlation estimated by Sarkar et al. (2006) from experimental results presented by Ortiz et al. (2003). The output pressure is assumed to be calculated by the high pressure control system in accordance with the hot water inlet temperature. For carbon dioxide transcritical cycles, there exists an optimal high pressure that gives a maximum COP (Lorentzen, 1994). The high pressure is given by a correlation from Liao et al. (2000). The isentropic efficiency of the CO_2 compressor is based on the correlation of Brown et al. (2002) who curve-fitted the results presented by Rieberer and Halozan (1998). The isentropic efficiency for R407C is calculated using a correlation based on curve-fitted results of experiments carried out in our laboratory on the Copeland ZB38KCE compressor (Fig. 8). Isentropic efficiency is higher for CO_2 because of the lower compression ratio. For the R407C model, the relative clearance volume is set to 2%. Mechanical and electrical efficiencies are respectively 0.8 and 0.95. These values are deliberately high in order to simulate

highly efficient compressors. Finally, the discharge temperature is calculated thanks to the Refprop database (2002) for the outlet values of enthalpy (Eq. (5)) and high pressure.

$$\eta_{vol} = 1 - c \cdot \left[\left(\frac{HP}{LP} \right)^{\frac{1}{n}} - 1 \right] \tag{1}$$

$$\dot{m} = \rho \cdot \eta_{vol} \cdot V_s \tag{2}$$

$$\dot{W}_{carnot} = \dot{m} \cdot \left(h_{o-ideal} - h_i \right) \tag{3}$$

$$\dot{W} = \frac{\dot{W}_{carnot}}{\eta_{is} \cdot \eta_{mec} \cdot \eta_{el}} \tag{4}$$

$$h_o = h_i + \frac{h_{o-ideal} - h_i}{\eta_{is}} \tag{5}$$

Frosting - defrosting model

Once the capacities are calculated, the frost mass variations on the air coil and the temperature variations of the cold tank are calculated using Eq. (6) to (9). The frost layer is assumed to be very thin and continuous so that it does not affect the cooling capacity. This implies that the cold tank water temperature varies rather quickly. The frosting-defrosting sequence lasts around 20 minutes. This rather short time of sequence ensures a low frosting level. x_L (= 0.25) is the estimated percentage of the cooling capacity used by frost formation in latent heat transfer. η_{df} (= 0.5) is the estimated efficiency of the defrosting system. This means that 50% of the cooling capacity is used to carry out defrosting. The frosting – defrosting sequence is modelled using a time step of 0.5 second. Fig. 9 shows the little influence (less than 5.4%) of parameters x_L, η_{df} and the time step value dt on the relative difference between the dual mode time ratios (Eq. (10) and (11)) of R407C and CO_2. The coupling of the parameters has also been investigated and does not affect further the ratio difference. The difference in the overall operation of the HFC and CO_2 heat pumps will only be very slightly affected by a variation of these parameters.

Frost mass variation during frosting:

$$\frac{dm_f}{dt} = \frac{\dot{Q}_c . x_L}{L_S} \tag{6}$$

Frost mass variation during defrosting:

$$\frac{dm_f}{dt} = -\frac{\dot{Q}_c.\eta_{df}}{L_F} \tag{7}$$

Cold tank temperature increase:

$$\frac{dT_{cs}}{dt} = \frac{\dot{Q}_{sc}}{m_w.Cp_w} \tag{8}$$

Cold tank temperature decrease:

$$\frac{dT_{cs}}{dt} = \frac{\dot{Q}_c}{m_w.Cp_w} \tag{9}$$

Time ratios were calculated in order to take into account the alternation of the two modes with and without frosting (Eq. (10) and (11)). These ratios are used in the coupling of the HPS with the building.

$$r_{DM-nof} = \frac{dual\ mode\ time\ without\ \ frosting}{time\ of\ \ the\ heating\ \ sequence} \tag{10}$$

$$r_{DM-f} = \frac{dual\ mode\ time\ with\ \ frosting}{time\ of\ \ the\ heating\ \ sequence} \tag{11}$$

A third time ratio was calculated to estimate the time of frosting conditions during each day of the year (Eq. (12)). It is assumed that frost appears when the ambient temperature is below 6°C. This assumption depends on the ambient air conditions. The value of this threshold is negligible for our comparison. It is a matter of component design.

$$r_{T<6°C} = \frac{Number\ of\ \ hours\ during\ \ which\ T_{amb} < 6°C}{24} \tag{12}$$

Operating strategy

The coupling of the HPS with the building is a simulation based on daily energy balances. For each day of the year, the heating and cooling demands and the heating and cooling capacities in each mode are confronted. The operating times per mode are obtained by dividing demands by capacities. The demands can be satisfied under several modes. The HPS starts to work in the dual mode as this mode is the most efficient. Then it continues in the heating or the cooling mode depending on the remaining thermal demands.

Domestic hot water production is not simulated in the same way for the HFC and CO_2 heat pumps. For the HFC heat pump, DHW production is carried out by the heat pump up to 40°C and then by an

electric auxiliary heater from 40 to 55°C. For CO_2, all the DHW demand is satisfied by the heat pump thanks to the progressive temperature decrease in the gas cooler.

The times of operation in each mode are calculated following the operating strategy. Dual mode is run first, until the minimum between heating and cooling demands are satisfied (Eq. (13)). The second part of the equation corresponds to the alternation between dual and heating mode during a heating period.

$$t_{DM} = \min\left(\frac{q_h}{\dot{Q}_{hDM}}, \frac{q_c}{\dot{Q}_{cDM}}\right) + \left[r_{T<6°C}.r_{DM-f} + \left(1 - r_{T<6°C}\right).r_{DM-nof}\right] \times \left[\frac{q_h - \dot{Q}_{hDM} \cdot \min\left(\frac{q_h}{\dot{Q}_{hDM}}, \frac{q_c}{\dot{Q}_{cDM}}\right)}{\dot{Q}_{hDM}}\right] \tag{13}$$

where q_h is the daily demand in heating, q_c, the daily demand in cooling and $\dot{Q}_{hDM}$, the heating capacity in dual mode.

In heating mode, the operating time is the time needed to cover all the heating needs minus the dual mode time.

$$t_{HM} = \left[1 - \left(r_{T<6°C}.r_{DM-f} + \left(1 - r_{T<6°C}\right).r_{DM-nof}\right)\right] \times \left[\frac{q_h - \dot{Q}_{hDM} \cdot \min\left(\frac{q_h}{\dot{Q}_{hDM}}, \frac{q_c}{\dot{Q}_{cDM}}\right)}{\dot{Q}_{hHM}}\right] \tag{14}$$

where $_{HM}$ stands for heating mode.

In cooling mode, the operating time is the time needed to cover all the cooling needs minus the time needed for cooling in the dual mode.

$$t_{CM} = \frac{q_c - \dot{Q}_{cDM} \cdot \min\left(\frac{q_h}{\dot{Q}_{hDM}}, \frac{q_c}{\dot{Q}_{cDM}}\right)}{\dot{Q}_{cCM}} \tag{15}$$

where $_{CM}$ stands for cooling mode.

Performance evaluation and electricity consumptions calculations

Three performance factors are used: the first law COP, the Carnot COP and the second law efficiency. The corresponding equations are reported in table 2.

The first law coefficients of performance are defined as the useful energies provided at the water heat exchangers divided by the electricity consumption of the compressor. During a heating mode, the heating energy provided at the water condenser is the only considered. During a cooling mode, the cooling energy provided at the water evaporator is the only considered. During the dual mode of an alternated winter

sequence, the cooling energy is not taken into account because it is not used for space cooling. If the heating and cooling capacities are useful in a dual mode, the first law coefficient of performance is given by the sum of heating and cooling COPs. The daily and annual coefficients of performance are calculated in proportion to the operating times per mode.

The Carnot COPs have also been calculated on each time step. The Carnot COPs in heating, dual and cooling modes are expressed in terms of temperatures of sources by the combination of first and second laws of thermodynamics and by imposing a zero entropy generation in the second law. The annual Carnot COP is calculated in proportion to the operating times obtained by the calculation using the first law COP.

Second law (exergy) efficiency is calculated using equations presented by Sarkar et al. (2004) as the ratio of the net exergy output to the work input to the compressor. Exergy outputs are calculated for the useful heat exchangers.

Electricity consumptions are deduced from the daily calculations. They include the consumption of an eventual auxiliary heater for DHW production. The consumptions of other auxiliaries like fans, pumps or control equipment are not taken into account.

Hypotheses for standard heat pumps

The calculations were also carried out for standard reversible HFC and CO_2 heat pumps that have the same heating and cooling capacities as the HFC and CO_2 HPSs: the standard heat pump models have the same steady state performances depending on the temperature than the ones calculated for the HPS. During summer, the standard heat pumps are supposed to be in a cooling mode and so, not to be able to produce domestic hot water. All the heat needed for this purpose is then provided by the electric heater. The defrosting sequence is supposed to last the same time for both machines. This means that the dual mode time of the HPS equals the defrosting time of the standard heat pump. At first this assumption seems penalizing for the standard heat pump but it gives actually a fair estimation of the performance loss during defrosting. The standard heat pump is supposed to use a reversed cycle defrosting method. So there is a loss of performance due to two contributions: the shutdown of heat production and the drawing on the stock for space heating for the evaporation of the reversed cycle. The electricity consumption of a standard heat pump in a heating mode is given by Eq. (16).

$$C_{standard\ HP} = \left(1 + r_{T<6°C} \cdot r_{DM-f}\right) \cdot \frac{q_h}{COP_{HM}} \tag{16}$$

4. Results and discussion

Building simulation

The annual simulation of the hotel shows the variation of daily heating and cooling demands all year round (Fig. 10). Annual needs amount to 25 322 kWh for DHW production, 68 640 kWh for space heating and 30 146 kWh for space cooling. A heat pump of 50 kW heating capacity is installed in the building to satisfy these needs.

It can also be pointed out that during spring and autumn heating and cooling demands appear during the same days. During summer the plateau in the heating curve corresponds to the domestic hot water demand and is quite constant. From the end of April to the end of October a significant part of the total heating and cooling needs can be satisfied by a simultaneous production.

Steady state performance

Fig. 11 shows the first law COPs, the Carnot COPs and the second law efficiencies calculated in steady state simulations in the heating mode for lower air temperatures, in the cooling mode for higher air temperatures and in the dual mode for an average temperature of 20°C. The heating mode is less efficient for CO_2 than for R407C from 18% at -15°C to 43% at 15°C. The CO_2 cooling mode is 28% less efficient at 40°C but 7% more efficient at 25°C. The dual mode is 22% less efficient in terms of a COP integrating heating and cooling energies at an ambient temperature of 20°C. The dual mode is also used at other ambient temperatures. Additional calculations showed a heating and cooling integrated first law coefficient of performance decrease of between 43% at -15°C and 15% at 15°C. These results are based only on the thermodynamic cycles. CO_2 is clearly less efficient in terms of first law COP than R407C when used in classic space heating or cooling applications. The standard heat pump models also use these first law COPs in the coupling with the building. The Carnot COPs are based on temperatures of sources. The difference between HFC or CO_2 COPs and Carnot COPs represent the degree of irreversibility within each cycle. It seems clear that the carbon dioxide transcritical cycle introduces more irreversibilities than the standard HFC refrigeration cycle.

The second law efficiency curves are linked to output energies and mean source temperatures. CO_2 values are between 25.8% and 12.0% in heating and 24.4% and 28.3% in cooling. R407C values are between 38.1% and 30.8% in heating and 25.9% and 34% in cooling. Globally carbon dioxide second law efficiency shows a little less dependency to temperature than R407C. At 25°C in cooling mode, first law

COP and second law efficiency are higher for CO_2 than for R407C. This tendency is in accordance with some results published by Kim et al. (2004). In dual mode, CO_2 is nearly as efficient as R407C in terns of exergy (42.0% for CO_2 and 45.3% for R407C).

Frosting – defrosting model

Time ratios were calculated according to Eq. (9) and (10) (Table 3) and proved different with and without frosting because they depend on the cooling capacity. The dual mode time ratio is quite near 15% for both fluids when there is frosting conditions. The defrosting acts upon the refrigerant like a subcooling. Therefore, there is an additional capacity at heat rejection that is compensated by an additional cooling capacity at the evaporator. Nevertheless the carbon dioxide HPS works longer under the dual mode than the R407C HPS, especially when there is no frosting: 0.166 for R407C against 0.221 for CO_2. This can be explained by the higher amount of energy recoverable by subcooling. This characteristic shortens the time of temperature rise between 5 and 15°C in the cold tank during the heating mode. Therefore the dual mode time takes a greater part of the sequence. The coefficients of performance are higher when operating on a dual mode because of the higher temperature source at the evaporator. A higher COP during a longer time in dual mode increases the average COP. The CO_2 HPS takes more benefit from the alternated sequence than the HFC HPS.

Annual performance

Table 4 presents first law COPs, Carnot COPs and second law efficiencies for R407C and carbon dioxide. The first law COP corresponds to the ratio of overall useful thermal energy to used energy. As expected, CO_2 has a lower first law COP than R407C. However, the HPS annual first law COPs are 3.57 for R407C and 3.26 for carbon dioxide which corresponds to a 8.7% reduction whereas the steady state performance calculations led to an average larger difference. This means that, considering the whole system operation and not only the steady state COPs, the decrease in performance between R407C and CO_2 becomes lower because of the higher subcooling energy. This conclusion is confirmed by the Carnot COPs that depend only on the times of operation in the different modes and by the operating strategy concerning alternated winter sequences between heating and dual modes and DHW production. Globally, Carnot COP is higher for CO_2 than HFC because of the enhanced use of the dual mode. The annual Carnot COPs are 11.06 for R407C and 12.10 for CO_2. Second law efficiencies also follow this tendency.

Using carbon dioxide, the dual mode operates during a longer time than with a HFC when running the winter alternated sequences and producing DHW during summer.

When compared to a standard heat pump, the R407C HPS proved more efficient in terms of first law COP and second law efficiency. However the annual Carnot COP is lower because of the lower source temperature in a dual mode than in a heating mode with an ambient temperature higher than 10°C, which occurs rather often under the climatic conditions of Paris. The CO_2 HPS shows an improvement in first law COP, Carnot COP and second law efficiency compared to a standard heat pump thanks to the enhanced operation in the dual mode.

Electricity consumptions

The electricity consumptions of the HPS and of a standard reversible heat pump using HFC or CO_2 are detailed on Table 5. Because of the type of climate of Paris, colder during winter than hot during summer as far as thermal demands are concerned, each system consumes more electricity in the heating mode than in the cooling mode. Comparing heat pumps to HPSs, it can be observed that the use of the dual mode, producing simultaneously hot and cold water, diminishes the electricity consumptions of the heat pumps in heating and cooling modes and of the auxiliary heater. During winter, part of the heating demand is satisfied with COPs improved by alternating heating and dual modes. During spring and autumn, depending on the major thermal demand, “free” cooling or “free” heating is performed in the dual mode. The auxiliary heater consumption is also lower for the HPS because during summer, the DHW is partly (or completely for CO_2) produced in a dual mode while for the standard heat pump, switched in a cooling mode for the hot season, it is entirely produced by the electric heater. Therefore electricity consumptions in heating, cooling and dual modes of the HPSs are lower than that of the heat pumps in heating and cooling modes. The HPS working with R407C consumes 16.6% less electricity than a standard heat pump. With carbon dioxide, the improvement reaches 27.4% thanks to the direct DHW production and to the favourable winter alternated sequence. The electricity consumption of the CO_2 HPS is lower than that of the HFC standard heat pump. The replacement of a standard heat pump by a HPS leads to a higher increase in performance with carbon dioxide than with a HFC.

TEWI calculations

The Total Equivalent Warming Impact (TEWI) is calculated for the four heat pump systems (Table 6) using the greenhouse gas emission ratio of electricity production of France (0.13 kg_{CO2}/kWh). The

refrigerant charge of the HPS is higher than that of a standard heat pump because of the implementation of a variable volume receiver, a secondary condenser and a subcooler at high pressure. A R407C HPS prototype having a heating capacity of 15 kW is currently under testing. Its refrigerant charge amounts to 9 kg whereas the conventional charge ratio would be around 0.2 kg per kW in heating. The refrigerant charge of the 50 kW R407C and CO_2 HPSs and standard heat pumps is respectively 18 kg and 6 kg. For a life time of 20 years, a leakage rate of 3% per year and a recovery rate of 75%, the TEWI is lower for the HPSs than for the standard heat pumps even if the refrigerant charge is increased. The savings in energy consumption have a much more significant impact than the increase of the refrigerant charge. The carbon dioxide HPS has the lowest TEWI with 95 359 kg of CO_2. There is a relative environmental benefit to use carbon dioxide instead of R407C as a working fluid for this concept of HPS with a saving of around 4 000 kg of CO_2, which represents 4% of the total equivalent warming impact.

5. Conclusion

A Heat Pump for Simultaneous heating and cooling has been designed in the aim of heating and cooling luxury dwellings, hotels and smaller office buildings and also producing domestic hot water. Running costs and greenhouse gas emissions can be diminished by using the same electric energy to produce hot and cold water simultaneously. This machine also proposes an answer to reduce the performance loss of air-to-water heat pumps under low ambient temperatures and especially during defrosting sequences by alternation between an air evaporator and a water evaporator.

The HPS has been designed for HFCs and CO_2. The results are obtained for highly efficient compressors and perfect heat exchangers and are closely linked to these assumptions. Today, HFCs are the most efficient and “secure” fluids on the market but they are greenhouse gases. Carbon dioxide is environmentally friendly but it is less efficient and its technology needs more development to be really competitive in space heating applications (Kim et al., 2004). Nevertheless its thermodynamic properties enable domestic hot water production. The alternated winter sequence offers a new solution for defrosting. Especially, it increases the average performance in heating, and increases further with a high subcooling capacity available with CO_2. The CO_2 HPS outperforms the HFC standard heat pump in terms of first law COP and annual electricity consumption and this opens the door to carbon dioxide as a working fluid for space heating applications. The properties of the carbon dioxide transcritical cycle

enhance the operation of the HPS in the dual mode as shown through the Carnot COP and second law efficiency annual values.

TEWI calculations conclude to a reduction of green house gas emissions by the use of carbon dioxide instead of R407C as a working fluid for this concept of HPS. Also, the environmental analysis could be extended to the life cycle cost (LCC) which could advantage more carbon dioxide because of the difference between the synthesis of R407C and the capture of CO_2 and because of smaller (thus probably cheaper in terms of CO_2 emissions) components for CO_2.

In conclusion, transcritical CO_2 technology is improving day after day and offers a slightly lower impact on global warming. However, HFC heat pumps for space heating and cooling still remain more efficient and less costly in terms of energy consumption.

References

ASHRAE Handbook, Fundamentals, 1989, 4.2-4.3.

Bennett, D. L., Chen, J. C., Forced convection boiling in vertical tubes for saturated pure components and binary mixtures, Journal of AIChE, 1980, Vol 26, 454-461.

Brown, J., S., Yana-Motta, S., F., Domanski, P., A., Comparative analysis of an automotive air conditioning system operating with CO_2 and R134a, International Journal of Refrigeration, 2002, Vol 25, 19–32.

Haberschill, P., Guitari, I., Lallemand, A., Comportement dynamique d'une pompe à chaleur au CO_2 en cycles sous critique et transcritique, International Journal of Refrigeration, 2002, Vol 25-4, 421-427.

Kim, M.-H., Pettersen, J., Bullard, C. W., Fundamental process and system design issues in CO_2 vapour compression systems, Progress in Energy and Combustion Science, 2004, Vol 30, 119-174.

Kusakari, K., The spread situation and the future view of the CO_2 refrigerant heat pump water heater in Japan, 7th IIR Gustav Lorentzen Conference, 2006, Trondheim, keynote speech.

Liao, S. M., Zhao T. S., Jakobsen A., A correlation of optimal pressures in transcritical carbon dioxide cycles, Applied Thermal Engineering, 2000, Vol 20, 831-841.

Liu, D., Zhao, F.-Y., Tang, G.-F., Frosting of heat pump with recovery facility, Renewable Energy, 2007, Vol 32, 1228-1242.

Lorentzen, G., Revival of carbon dioxide as a refrigerant, International Journal of Refrigeration, 1994, Vol 17-5, 292-301.

Lorentzen, G., The use of natural refrigerants: a complete solution to the CFC/HCFC predicament, International Journal of Refrigeration, 1995, Vol 18-3, 190-197.

Meunier, F., Rivet, P., Terrier, M.-F., Froid Industriel, Editions Dunod, 2005, 20-42, 305-312.

Nekså, P., CO_2 heat pump systems, International Journal of Refrigeration, 2002, Vol 25-4, 421-427.

Nekså, P., CO_2 as refrigerant, a way to reduce greenhouse gas emissions, 9th international IEA Heat Pump Conference, 2008, Zürich, Switzerland.

Ortiz, T., M., Li, D., Groll, E., A., Evaluation of the performance potential of CO2 as a refrigerant in air-to-air air conditioners and heat pumps: system modelling and analysis, ARTI Final Report, No. 21CR/610-10030, 2003.

Protocole de Kyoto à la convention-cadre des nations unies sur les changements climatiques, 1997.

REFPROP, Reference Fluid Thermodynamic and Transport Properties, NIST Standard Reference Database 23, Version 7.0, Copyright 2002.

Rieberer, R., Halozan, H., CO_2 heat pumps in controlled ventilation systems, IIR Gustav Lorentzen Conference, Oslo, Norway, 1998, p 212-222.

Sarkar, J., Bhattacharyya, S., Ram Gopal, M., Simulation of a transcritical CO_2 heat pump cycle for simultaneous cooling and heating applications, International Journal of Refrigeration, 2006, Vol 29, 735–743.

Stene, J., Residential CO_2 heat pump system for combined space heating and hot water heating, International Journal of Refrigeration, 2005, Vol 28, 1259-1265.

Solar Energy Laboratory, University of Wisconsin-Madison, TRNSYS, A Transient Simulation Program, 2000, Volume I, Reference Manual.

White, S., D., Cleland, D., J., Cotter, S., D., Stephenson, R., A., Kallu, R., D., S., Fleming, A., K., A heat pump for simultaneous refrigeration and water heating, IPENZ transactions, Vol 24, No. 1/EMCh, 1997.

Xia, Y., Zhong, Y., Hrnjak, P.S., Jacobi, A.M., Frost, defrost, and refrost and its impact on the air-side thermal-hydraulic performance of louvered-fin, flat-tube heat exchangers, International Journal of Refrigeration, 2006, Vol 29, 1066-1079.

Zhao, Y., Ohadi, M., M., Radermacher, R., Microchannel heat exchangers with carbon dioxide, ARTI Final Report, No. 21CR/10020-01, 2001.

List of figures

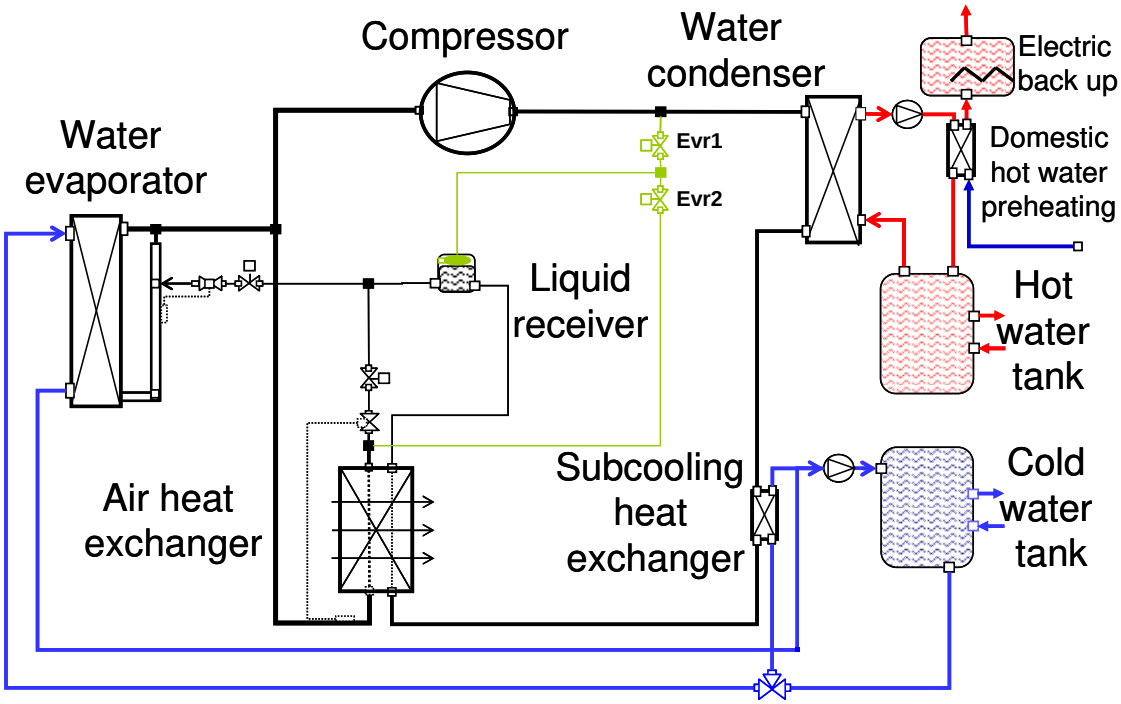

Fig. 1 – Schematic layout of the HFC HPS

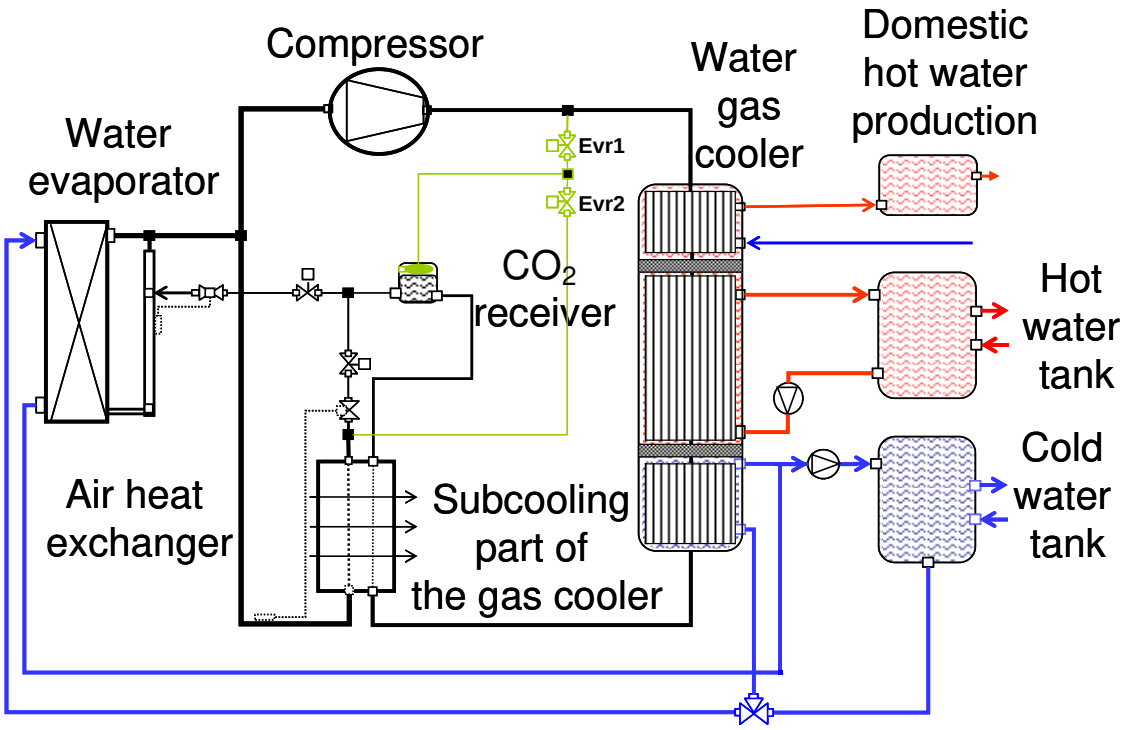

Fig.2 – Schematic layout of the CO_2 HPS

Fig. a1 **Heating mode, HFC**

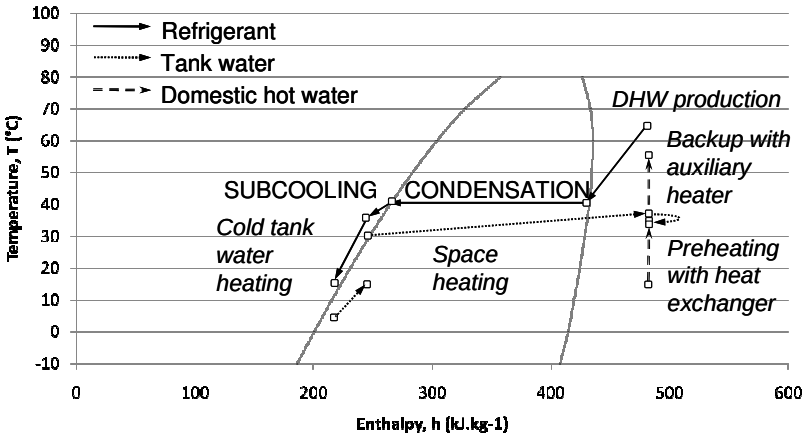

Fig. a2 **Winter dual mode, HFC**

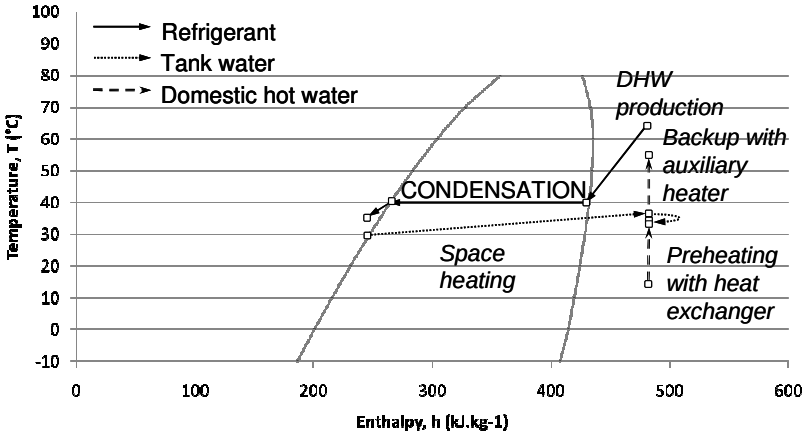

Fig. a3 **Summer dual mode, HFC**

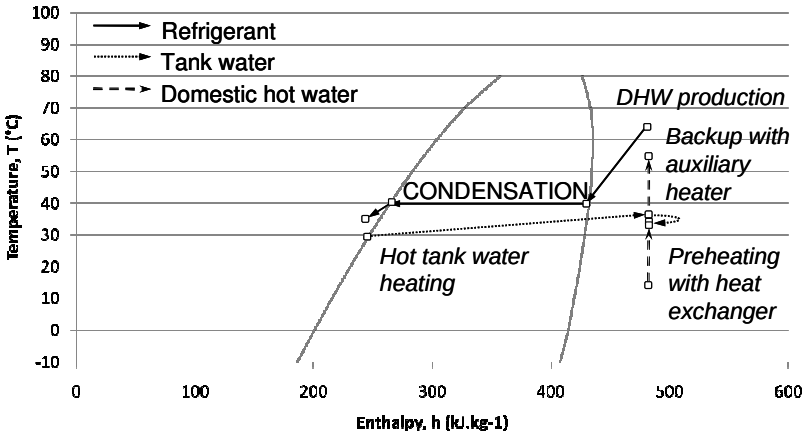

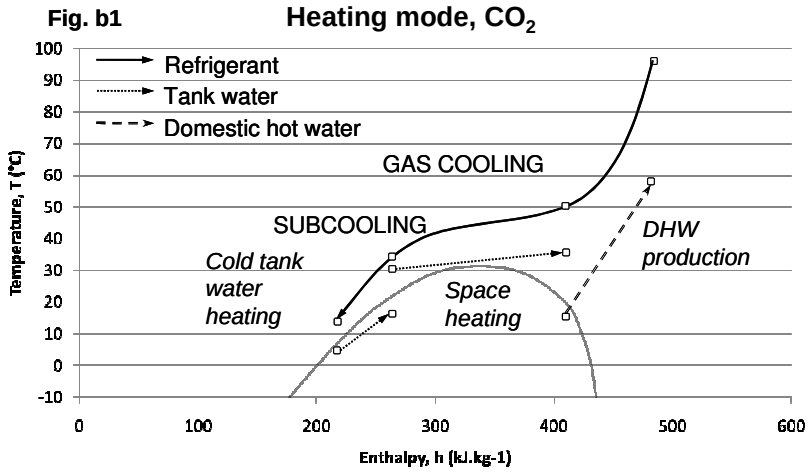

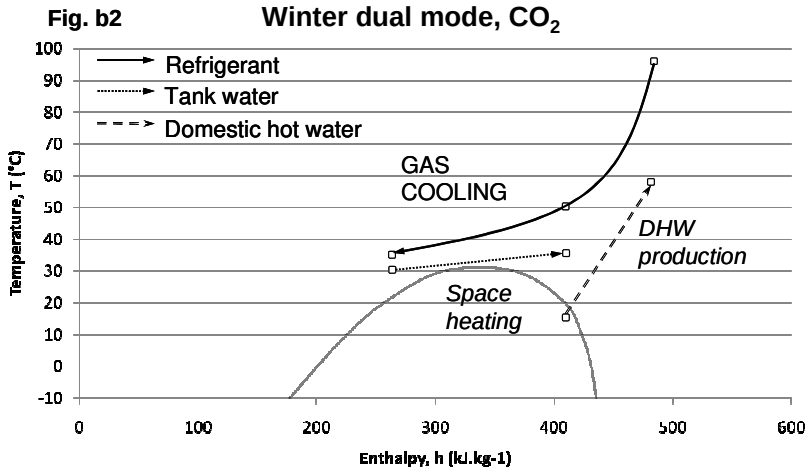

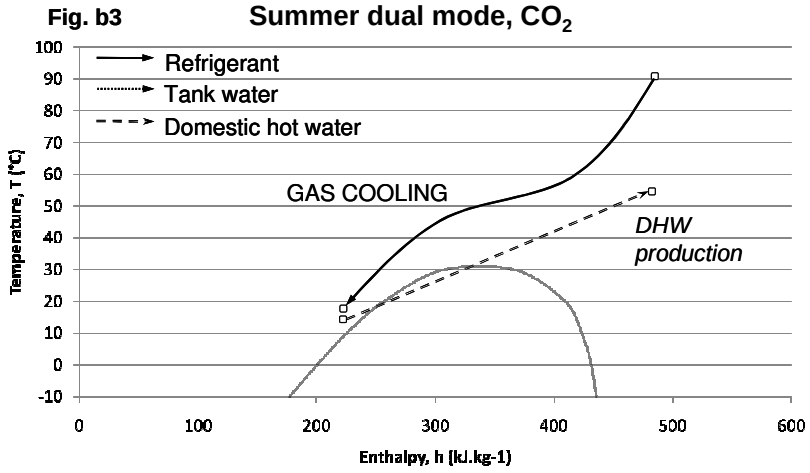

Fig. 3 – Illustration of the heat production processes for HFC and CO_2 heat pumps in heating mode and dual mode during winter and summer

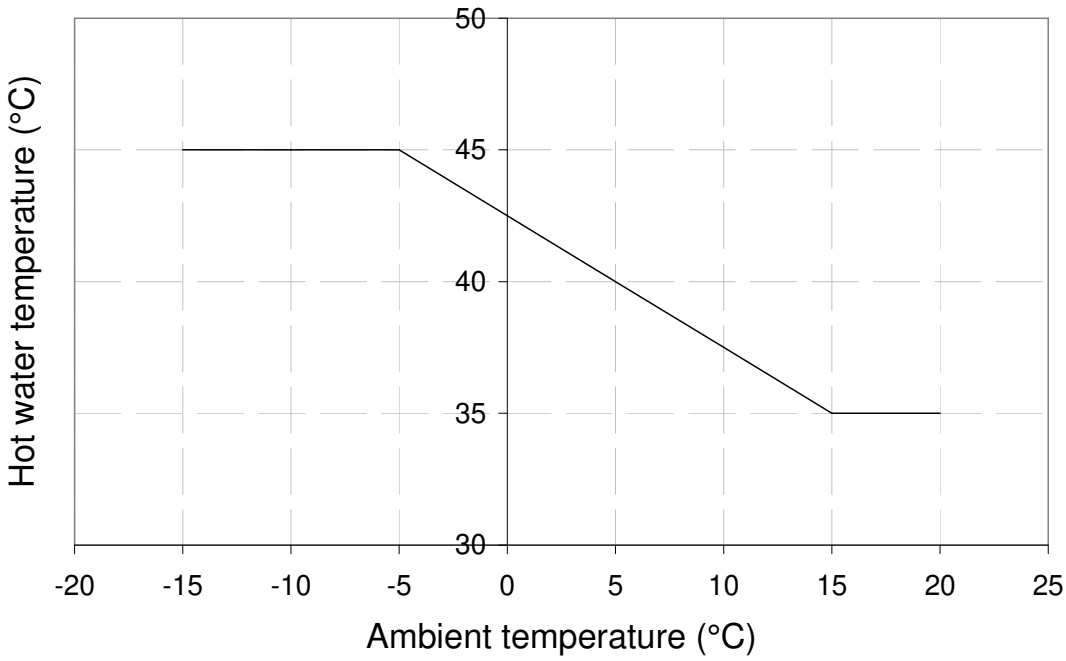

Fig. 4 – Set point curve for hot water for space heating depending on ambient temperature

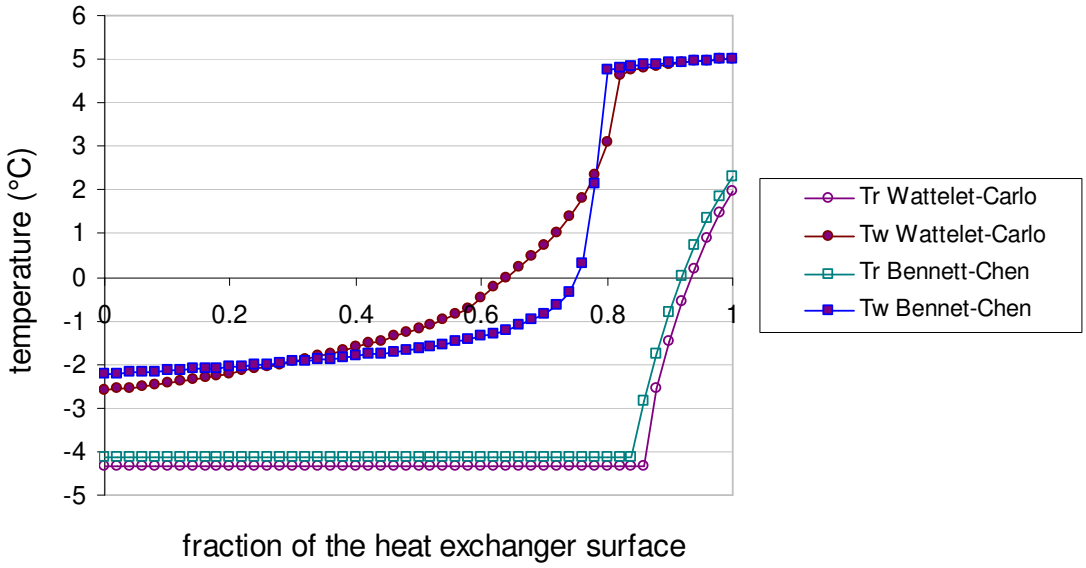

Fig. 5 – Calculation of the temperatures along a CO_2 evaporator using Bennett-Chen and Wattelet-Carlo correlations

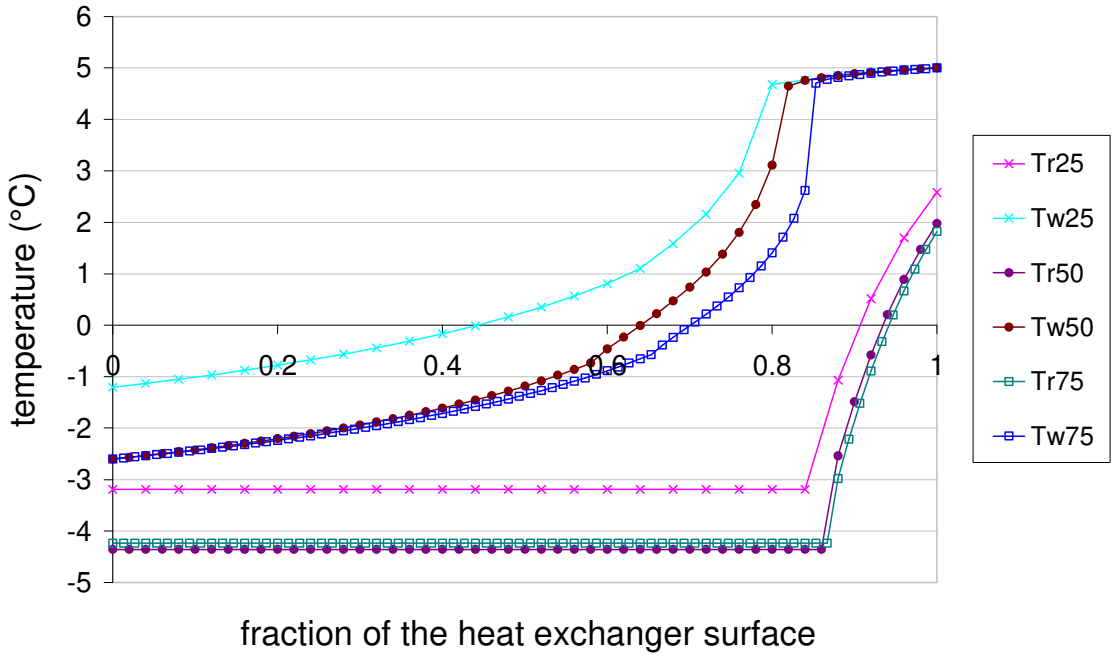

Fig. 6 – Influence of the number of sections on the water (from Tw25 to Tw75) and refrigerant (from Tr25 to Tr75) temperature calculation along a CO_2 evaporator

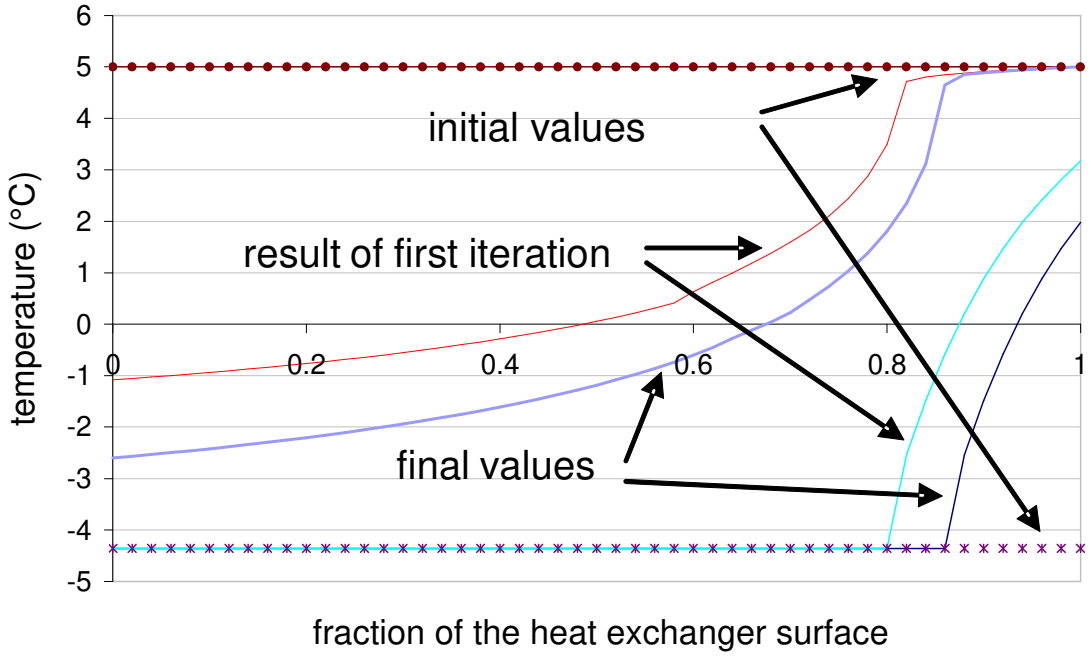

Fig. 7 – Illustration of the temperature calculation strategy on a 50-section CO_2 evaporator

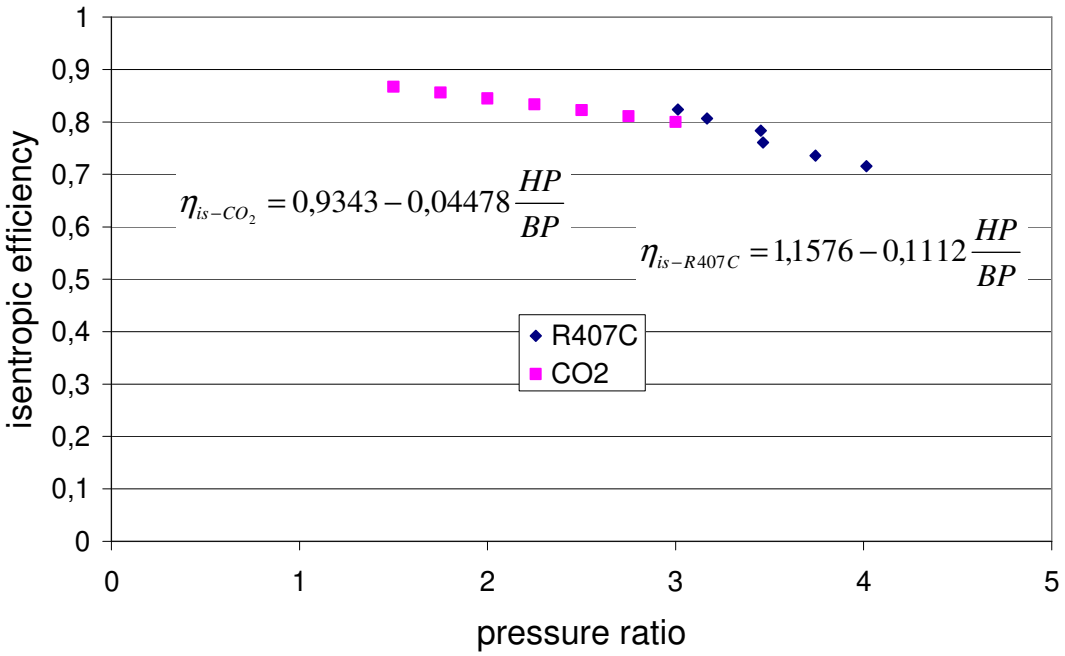

Fig. 8 – Isentropic efficiency vs. pressure ratio for CO_2 and R407C and curve-fitted equations

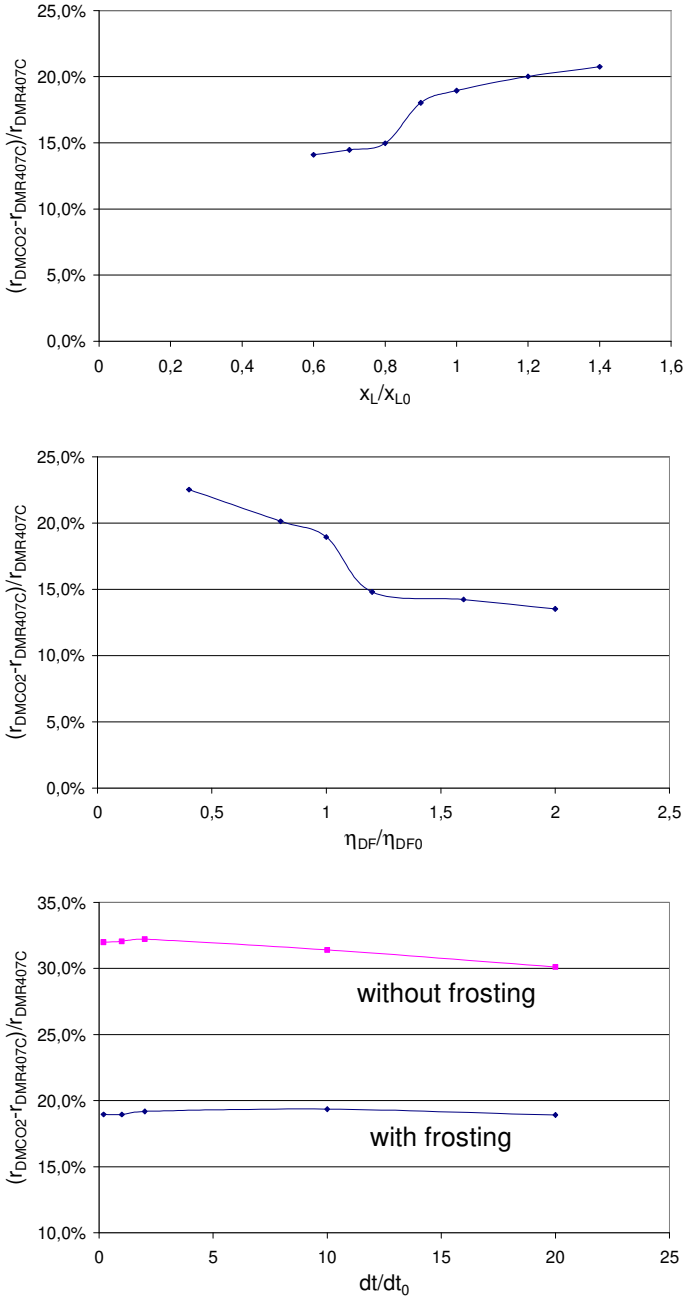

Fig. 9 – Influence of parameters x_L and η_{DF} and the simulation time step dt on the difference between the HFC and CO_2 dual mode time ratios

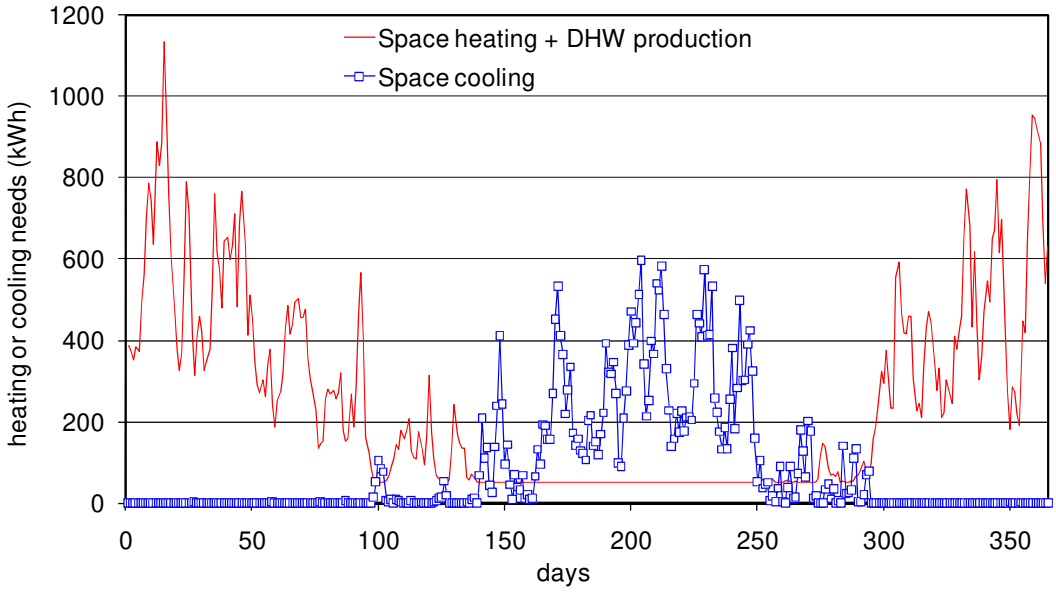

Fig. 10 – Daily needs in heating and cooling of a 45 bedrooms hotel in Paris

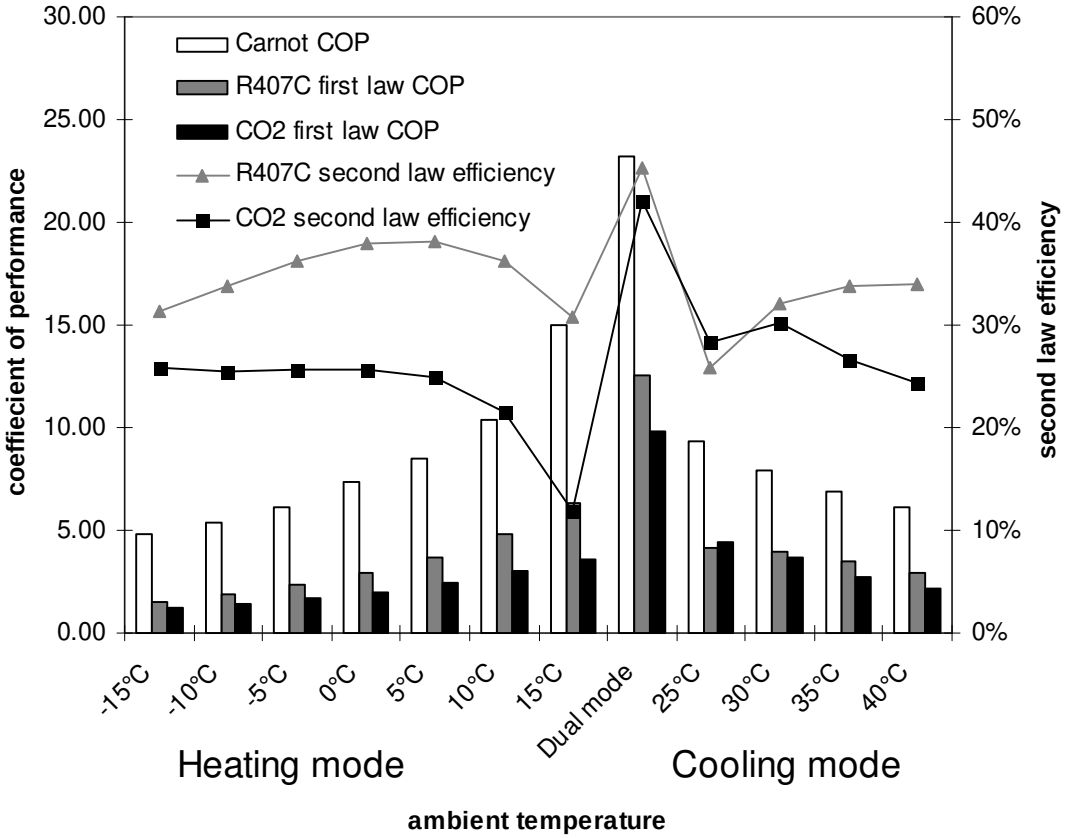

Fig. 11 – First law and Carnot coefficients of performance and second law efficiency in heating, cooling and dual modes depending on temperature (20°C corresponding to dual mode)

List of tables

Table 1 – Heat exchanger models characteristics of the 50 kW heating capacity HPS and standard heat pumps based on existing components

System	Refrigerant	Secondary fluid	Heat exchanger	Heat transfer area (m^2)
HPS	R407C	Water	Condenser	8.51
		(plate heat exchanger)	Subcooler	2.84
			Evaporator	2.78
		Air	Condenser	14.72
		(air coil)	Evaporator	14.72
	CO_2	Water	Gas cooler DHW heating	2.84
			Gas cooler space heating	5.10
			Subcooler	2.84
			Evaporator	2.78
		Air	Gas cooler	14.72
			Evaporator	14.72
Standard heat pump	R407C	Water	Condenser / Evaporator	5.10
		Air	Condenser / Evaporator	14.72
	CO_2	Water	Condenser / Evaporator	5.10
		Air	Condenser / Evaporator	14.72

Table 2 – Heat exchanger models characteristics of the 50 kW heating capacity HPS and standard heat pumps based on existing components

Performance factor	Heating mode	Cooling mode	Dual mode
First law COP	$\frac{Q_h}{W}$	$\frac{Q_c}{W}$	$\frac{Q_h + Q_c}{W}$
Carnot COP	$\frac{T_{hot\ source}}{T_{hot\ source} - T_{cold\ source}}$	$\frac{T_{cold\ source}}{T_{hot\ source} - T_{cold\ source}}$	$\frac{T_{hot\ source} + T_{cold\ source}}{T_{hot\ source} - T_{cold\ source}}$
Second law efficiency	$\frac{Q_h}{W} \cdot \left\lvert 1 - \frac{T_o}{\overline{T}_{cold\ source}} \right\rvert$	$\frac{Q_c}{W} \cdot \left\lvert 1 - \frac{T_o}{\overline{T}_{hot\ source}} \right\rvert$	$\frac{Q_h}{W} \cdot \left\lvert 1 - \frac{T_o}{\overline{T}_{cold\ source}} \right\rvert + \frac{Q_c}{W} \cdot \left\lvert 1 - \frac{T_o}{\overline{T}_{hot\ source}} \right\rvert$

Table 3 – Time ratios of the dual mode with and without frosting during winter alternated sequences

Time ratio	R407C	CO_2
$r_{DM\text{-}nof}$	0.166	0.221
$r_{DM\text{-}f}$	0.145	0.165

Table 4 – Annual first law COP, Carnot COP and second law efficiency of a HPS and a reversible heat pump working with R407C or carbon dioxide

System	Refrigerant	First law COP	Carnot COP	Second law efficiency
HPS	R407C	3.57	11.06	26.40%
	CO_2	3.26	12.10	27.48%
Standard	R407C	3.06	11.49	23.78%
heat pump	CO_2	2.70	10.95	18.38%

Table 5 – Electricity consumption (kWh) in different modes, for a HPS and a reversible heat pump, and for R407C and carbon dioxide

Fluid	HFC		CO_2	
System	HPS	standard heat pump	HPS	standard heat pump
cooling mode	5 031	5 946	4 593	5 604
heating mode	16 750	21 573	26 343	36 634
dual mode	3 959	0	5 739	0
auxiliary heater for DHW	9 536	14 753	0	8 248
total	35 275	42 272	36 675	50 487

Table 6 – TEWI calculation for the R407C and CO_2 HPSs and standard heat pumps

Type of heat pump	Electricity consumption (kWh)	Refrigerant charge (kg)	GWP_{100} (kg CO_2)	Direct Warming Impact (kg CO_2)	Indirect Warming Impact (kg CO_2)	TEWI (kg CO_2)
R407C HPS	35 275	18	1 526	7 783	106 118	99 498
R407C HP	42 272	6	1 526	3 205	123 950	113 112
CO_2 HPS	36 675	18	1	5	127 942	95 359
CO_2 HP	50 487	6	1	2	162 428	131 267